

Effects of annealing of poly(3-hexylthiophene) film on the performance of double-layered EL devices of ITO/polymer/Alq3/Mg-Ag

Joji Ohshita,^{a,*} Yosuke Tada,^a Atsutaka Kunai,^{a,*} Yutaka Harima,^a Atsushi Kohno,^{b,*} Yoshihito Kunugi^c

^a*Department of Applied Chemistry, Graduate School of Engineering, Hiroshima University, Higashi-Hiroshima 739-8527, Japan*

^b*Department of Applied Physics, Faculty of Science, Fukuoka University, 8-19-1 Nanakuma, Jonan-Ku, Fukuoka 814-0180, Japan*

^c*Department of Applied Chemistry, Faculty of Engineering, Tokai University, 1117 Kitakaname, Hiratsuka , 259-1292, Japan*

Abstract

Double layer devices with a structure of ITO/pHT/Alq3/Mg-Ag (ITO = indium tin oxide, pHT = regio-regular or random poly(3-hexylthiophene), Alq3 = tris(8-hydroxyquinoline)aluminium) were fabricated. The device with a random pHT film emitted a green-yellow light in all voltage region, while that having a regio-regular pHT film exhibited a color change from green to red by applying the bias voltage higher than 15 V. Annealing the pHT films prepared on ITO at 200°C for 1 h in nitrogen, prior to vapor-deposition of the Alq3 layer, improved the device performance with lowering the onset bias voltage by 2-3 V. The EL colors and spectra were also affected by annealing. X-ray reflectivity measurements before and after annealing the pHT film on ITO indicated increased density of the pHT layer and structural changes in the

* Corresponding authors

E-mail: jo@hiroshima-u.ac.jp (J. Ohshita), akunai@hiroshima-u.ac.jp (A. Kunai), kohno@fukuoka-u.ac.jp (A. Kohno)

pHT/ITO interface by annealing, which seems to be responsible for the improved EL device performance.

Key words: Polythiophene, Regio-regularity, Hole-transport, EL device, Annealing, Interface, X-ray reflectivity

1. Introduction

Since the first electroluminescence (EL) from devices with a conjugated polymer film was reported [1], many efforts have been made to improve and control the EL performance leading to, for example, lower turn-on voltages, higher luminance, and color-tuning. One of the most effective and simple methods to improve or control the EL performance may be thermal treatment of the polymer film. Improved performance of poly(phenylenevinylene)-based EL devices by heating the polymer film prepared on an electrode has been reported [2,3]. Similar improvement of the EL performance by annealing thiophene-based emitting polymer films also has been reported [4]. Effects of heat treatment of urethane-substituted-polythiophene/Alq₃ double layer devices have been studied and emission color changes accompanied with quantum efficiency enhancement by heating the devices were reported [5]. In these studies, it has been proposed that the effects of thermal treatment of polymer films on the EL properties may be ascribed to the structural changes in the interfaces between the polymer layer and electrodes as well as between polymer and Alq₃ layers in the double layer system. However, no direct evidences for the structural changes have been provided so far.

In the course of our studies concerning the functionalities of poly- and oligothiophene-based films [6], we found that annealing the polymer films significantly affected the EL color and performance of double layer devices with the structure of

ITO/(r- or ht-pHT)/Alq3/Mg-Ag, where r- and ht-pHT = regio-random and regular poly(3-hexylthiophene), and Alq3 = tris(8-hydroxyquinoline)aluminium. X-ray reflectivity (XRR) measurements before and after annealing the pHT film on ITO and the simulation of XRR provided evidences for increasing the density of the polymer film and a structural change of the pHT/ITO interface.

2. Experimental

2.1. Materials

Regio-random and regular poly(3-hexylthiophene) (r-pHT and ht-pHT), having head-to-tail linkage of 50-55% and >97%, respectively, were purchased from Aldrich Chemical Co. and used as obtained. Alq3 was obtained from Tokyo Kasei Kogyo Co. and purified by sublimation. Glass plates coated with ITO (indium tin oxide) and Mg-Ag alloy were obtained from Nippon Sheet Glass Co. and Rare Earth Metals Co., respectively.

2.2. Fabrication of EL devices.

A thin film (ca 150 nm) of r-pHT or ht-pHT was prepared by spin coating from the chloroform solution on an ITO electrode. An electron-transporting-emitting layer was then prepared by vacuum deposition of Alq3 at 1×10^{-5} torr with a thickness of 60-70 nm on the polymer film. Finally a layer of Mg-Ag alloy with an atomic ratio of 10:1 was deposited on the Alq3 layer surface as the top electrode at 1×10^{-5} torr. The emitting area was $0.5 \times 1.0 \text{ cm}^2$.

2.3. XRR measurements and analysis

A reflectometer with the Eulerian cradle and the graded multilayer mirror was set for XRR measurement (Philips: X'Pert PRO system). Incident X-ray (CuK α) came to the mirror through a divergence slit and was converted from the divergent beam into a

quasi-monochromatic and -parallel beam of high intensity by the mirror. A parallel-plate collimator, a receiving slit and a graphite monochromator were also attached before the detector. All the measurements were carried out at room temperature.

On the basis of the theory and the formulas of XRR from smooth or rough interfaces [7-10], calculation of XRR for multilayer model with rough interfaces and fitting to the experimental XRR curves were carried out for the quantitative analysis. The fitting parameters were thickness, density, and root mean square roughness in each layer.

3. Results and discussion

3.1. EL performance of ITO/pHT/Alq3/Mg-Ag devices

Figure 1 represents the current density-voltage (I-V) and luminance-voltage (L-V) characteristics of the devices with the structure of ITO/r- or ht-pHT/Alq3/Mg-Ag (devices r-I and ht-I). As can be seen in Figure 1, device r-I exhibited higher luminance than ht-I in the range of applied bias voltage of 7-17 V, although both of the devices showed essentially the same I-V characteristics. This seems to disagree with the fact that the improved regio-regularity usually enhances the conjugation in the polymer chain, and may be due to the different EL mechanism from these devices. Thus, as shown in Table 1 and Figure 2, device ht-I exhibited the EL maximum at 526 nm due to the Alq3 emission, while EL spectrum of r-I revealed two maxima at 519 and 598 nm, arising from the emissions from Alq3 and pHT layers, respectively. Interestingly, luminance of device ht-I increased in multi steps as increasing the bias voltage, including a rather slow increase at 8-13V and a rapid increase at 13-15 V, as shown in Figure 1. The luminance slightly decreased in the range of the applied voltage of 15-19 V, but again increased when the voltage exceeded 20 V. In addition,

EL color change from green to red ($\lambda_{\max} = 632$ nm) was observed around 15 V. At the voltages higher than 15 V, only the ht-pHT layer emitted the light and no emission bands were observed in the region shorter than 560 nm (Figure 2). In contrast to ht-I, the green-yellow color of the emission from device r-I did not change depending on the bias voltage and the EL spectra were always composed of the overlapping of the emissions from both Alq3 and r-pHT (Figure 2).

To examine the annealing effects, the polymer layer films prepared on ITO were annealed at 200°C for 1 h in nitrogen then Alq3 and Mg-Ag were vapor deposited on the resulting polymer surface to fabricate devices r- and ht-II. As can be seen in Figure 1, annealing the pHT film led to significant improvement of the device performance and lowered the onset bias voltage by 2-3 V for both devices r- and ht-II from those of r- and ht-I. Devices r- and ht-II emitted lights with $\lambda_{\max} = 531$ and 526 nm, respectively, indicating that only Alq3 layer emitted from both of the type II devices. No color and EL spectral changes depending on the applied voltage were observed for these devices. Interestingly, device r-II exhibited better performance than did ht-II as can be seen in Figure 1, although the reason is still unclear.

Table 1 also summarizes the optical changes of the polymer films on annealing. The polymer films became barely soluble in organic solvents by annealing. GPC analysis of the soluble parts of the annealed polymers showed large polydispersities of the molecular weights. These are indicative of that cross-linking reactions occurred on annealing. When polymer films prepared on quartz plates were heated under the same conditions as for the preparation of devices r- and ht-II, both the absorption and photoluminescence (PL) maxima moved to higher energies from those of the original ones. Presumably, cleavage of polymer backbone competed the cross-linking to some extent during the annealing process.

3.2. XRR Analysis of ht-pHT/ITO before and after annealing

XRR analysis is useful for structural study of thin films and the interfaces [7, 8]. In order to understand how annealing of pHT films affected the device performance, we carried out XRR measurements of the ht-pHT-coated ITO plates before and after annealing. The XRR spectra are plotted in Figure 3, together with the best-fitted curves calculated for a multilayered model, which consists of a bi-layer system of ITO, an interface layer, and a ht-pHT layer (Figure 4). The best fitted curves were obtained within least squares error $\chi^2 = 6.42 \times 10^{-2}$ and 7.29×10^{-2} for the data before and after annealing, respectively. The structural parameters for the best fit and their error ranges are listed in Table 2. Introduction of the bilayer model for ITO was necessary to obtain good agreement of the simulation. Indeed, good simulation fitting for XRR plots of the bare ITO glass plate without the covering polymer film, was also provided only by assuming a similar bi-layer model. The thickness of the ht-pHT layer was consistent with that evaluated from the cross-sectional scanning-electron-microscope (SEM) observations (Figure 5).

As shown in Table 2, density of ht-pHT layer was increased, presumably due to the cross-linking of the polymer chains. This would enhance the $\pi-\pi$ stacking in the polymer layer to improve its hole-transporting properties. It is also noted that thickness and density of the interface layer increased by annealing. Since no evident changes were observed in the surface roughness of the bare ITO plates by heating at 200°C by AFM measurements (Figure 6), it is likely that the increased thickness and density of the interface layer are ascribed to penetration of polymer materials into the ITO surface by annealing. The penetration seems to provide better adhesion of ITO/pHT to facilitate the hole-injection from ITO.

In conclusion, we demonstrated that annealing of the polythiophene films on ITO enhances the hole-transport of the film and/or hole-injection from the ITO electrode, although the polymer emission was suppressed by annealing. This seems to be due to the enhanced $\pi-\pi$ stacking in the films and improved adhesion of ITO/polymer layers,

as indicated by the XRR analyses.

Acknowledgments

We thank Tokuyama Science Foundation for financial support. We also thank Dr. Hiroshi Fukuoka (Graduate School of Engineering, Hiroshima University) for his assistance in SEM measurements.

References

- [1] J. H. Burroughes, D. D. C. Bradley, A. R. Brown, R. N. Marks, K. Mackay, R. H. Friend, P. L. Burns, A. B. Holmes, *Nature*, 347 (1990) 539.
- [2] (a) T. -W. Lee, O. O. Park, *Adv. Mater.*, 12 (2000) 801;
(b) T. -W. Lee, O. O. Park, L. -M. Do, T. Zyung, *Synth. Met.*, 117 (2001) 249.
- [3] J. H. Ahn, C. Wang, N. E. Widdowson, C. Pearson, M. R. Bryce, M. C. Petty, *J. Appl. Phys.*, 98 (2005) 054508.
- [4] (a) T. Ahn, H. Lee, S. -H. Han, *Appl. Phys. Lett.*, 80 (2002) 392;
(b) Y. H. Niu, Q. Hou, M. Yuan, Y. Cao, *Synth. Met.*, 135-136 (2003) 477;
- [5] S. -D. Jung, T. Zyung, W. H. Kim, C. J. Lee, S. K. Tripathy, *Synth. Met.*, 100 (1999) 223.
- [6] (a) X. Jiang, Y. Harima, K. Yamashita, Y. Tada, J. Ohshita, A. Kunai, *Chem. Phys. Lett.*, 364 (2002) 616;
(b) J. Ohshita, D.-H. Kim, Y. Kunugi, A. Kunai, *Organometallics*, 24 (2005) 4496.
- [7] E. Chason, “*In Situ Real-Time Characterization of Thin Films*” ed. by O. Auciello and A. R. Krauss, Chap. 6 (John Wiley & Sons, Canada, 2001) 167.
- [8] V. Holy, U. Pietsch, T. Baumbach, “*High-Resolution X-ray Scattering from Thin Films and Multilayers*”, (Springer-Verlag, Berlin, 2001).
- [9] L. G. Parratt, *Phys. Rev.*, 95 (1954) 359.

[10] S. K. Sinha, E. B. Sirota, S. Garoff, Phys. Rev. B38 (1988) 2297.

Table 1. Effects of annealing of pHT films on molecular weights and optical properties, and EL maxima form devices ITO/pHT/Alq₃/Mg-Ag

polymer		Mn (Mw/Mn) ^c	Absptn ^a	PL ^a	EL ^b	
			λ_{\max} [nm]	λ_{\max} [nm]	Device	λ_{\max} [nm]
r-pHT	as spin-coated	17 000 (2.6)	480	595	r-I	519, 598
	annealed	18 000 (3.6)	432	565	r-II	526
ht-pHT	as spin-coated	13 000 (1.5)	552	655	ht-I	526
	annealed	4500 (1.9)	475	600	ht-II	531

^a PL maximum of a spin-coated polymer film on a quartz plate.

^b EL maximum of the device at the bias voltage of 12V. At 15V, device ht-I emitted a light at $\lambda_{\max}= 632$ nm.

^c Determined by GPC, relative to polystyrene standards. For annealed polymer, only a soluble part was subjected to the analysis.

Table 2. Best fit parameters with error ranges for X-ray reflectivity spectra of ht-pHT films on ITO before and after annealing at 200°C for 1 h

layer (error range)	thickness/nm	roughness/nm	density/g·cm ⁻³
before annealing			
ITO-1	42.5 (42.4-42.5)	0.74 (0.63-0.85)	5.93 (5.91-5.95)
ITO-2	125.3 (124.8-125.7)	4.16 (4.13-4.19)	6.08 (6.06-6.10)
Interface	2.46 (2.40-2.51)	1.54 (1.51-1.56)	1.70 (1.69-1.72)
ht-pHT	147 (134-161)	5.7 (>3.3)	0.86 (0.85-0.87)
after annealing			
ITO-1	41.4 (41.3-41.5)	0.94 (0.61-1.02)	5.97 (5.93-6.01)
ITO-2	130.1 (129.2-130.9)	4.47 (4.38-4.55)	6.13 (6.09-6.16)
Interface	3.74 (3.67-3.81)	1.85 (1.82-1.88)	2.16 (2.13-2.19)
ht-pHT	154 (137-172)	5.7 (>3.2)	0.92 (0.90-0.94)

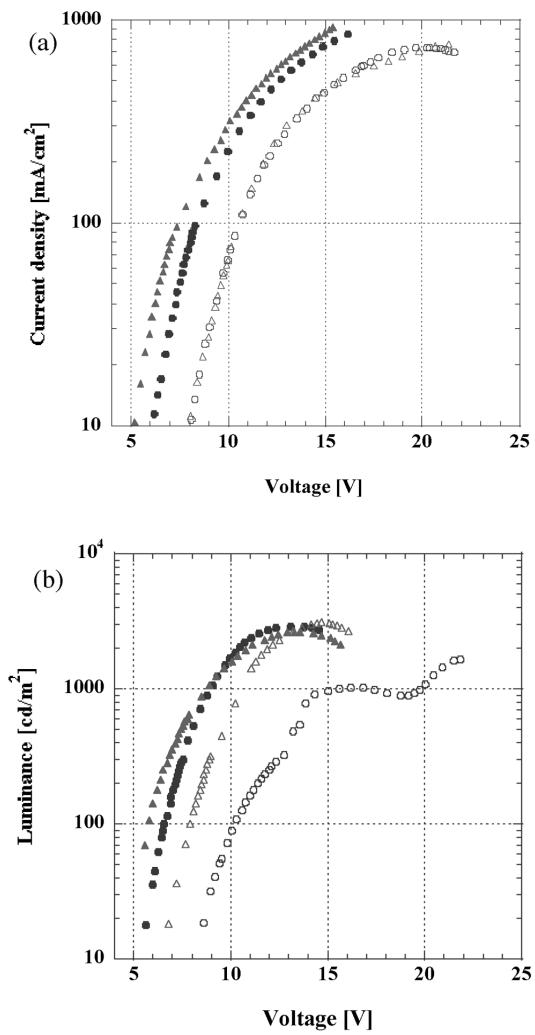


Figure 1. (a) Current density-voltage and (b) Luminescence-voltage plots for double layer EL devices having a polymer film of (Δ) r-pHT and (O) ht-pHT as prepared by spin-coating, r-I and ht-I, respectively, and (\blacktriangle) r-pHT and (\bullet) ht-pHT annealed, r-II and ht-II, respectively.

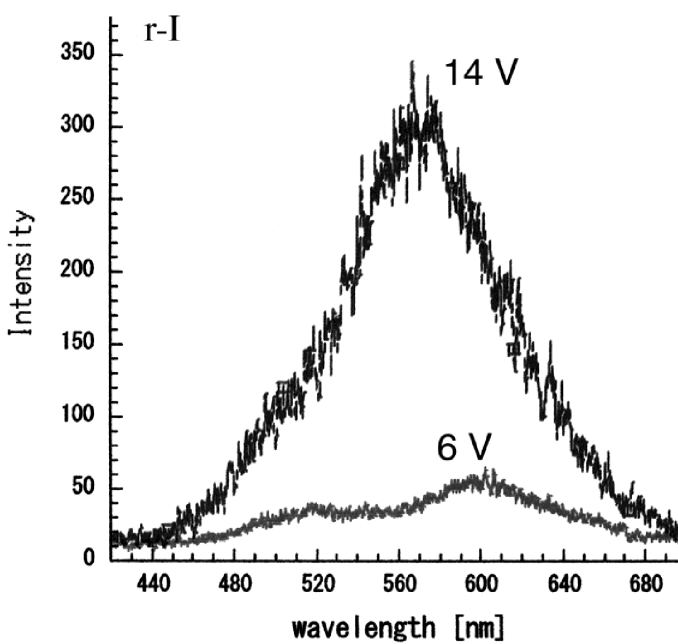
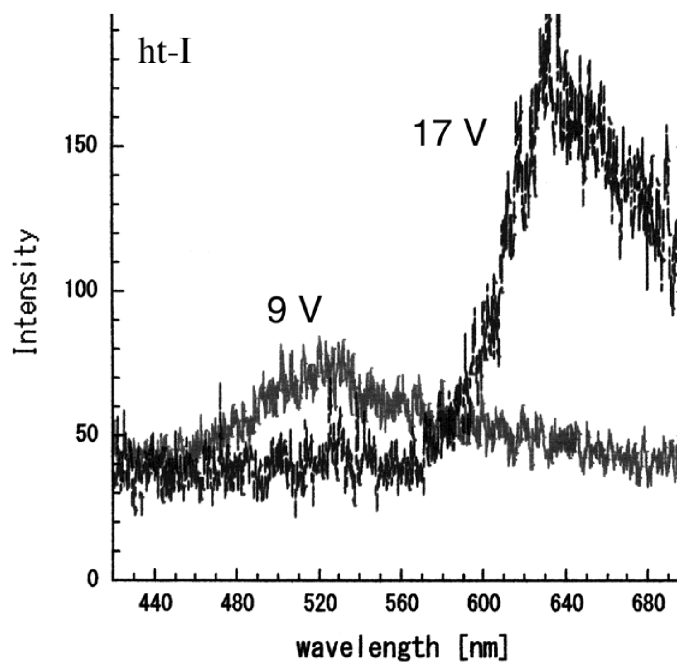


Figure 2. EL spectra from devices ht-I and r-I.

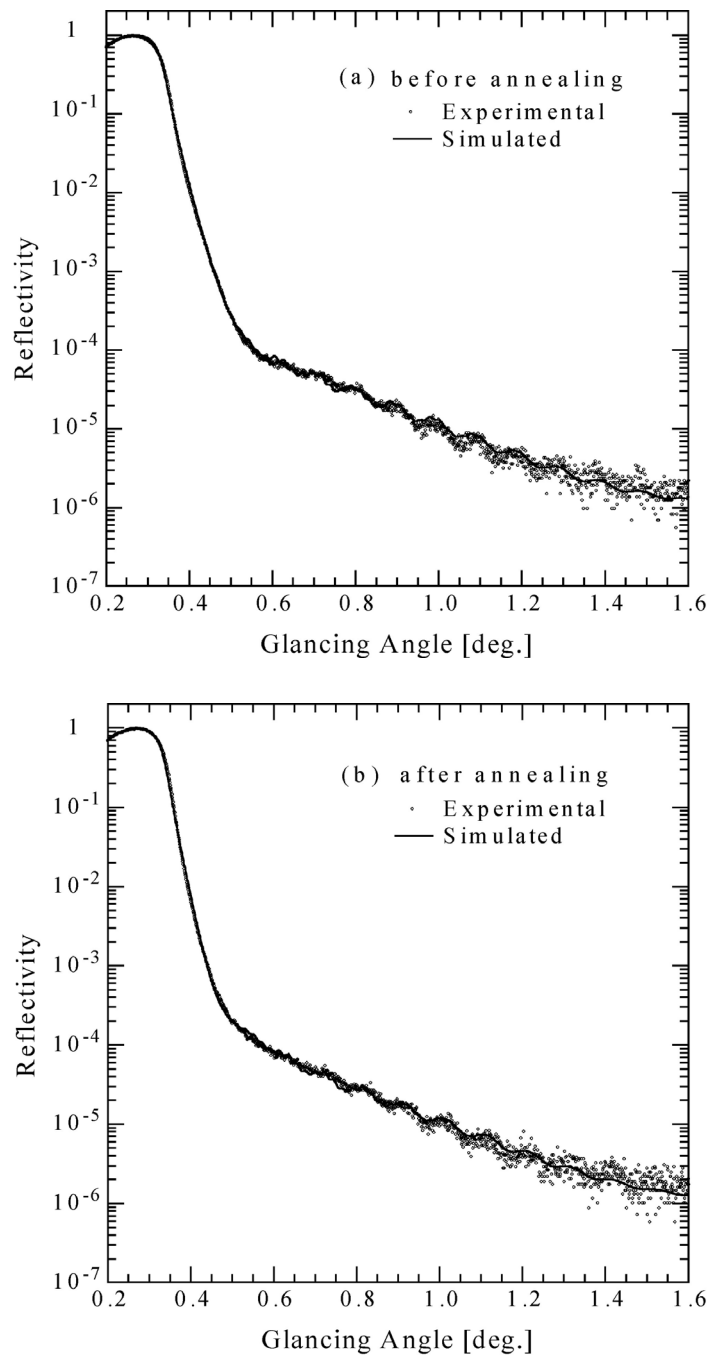


Figure 3. Experimental points and best-fit simulated curves of X-ray reflectivity for a ht-pHT film on ITO (a) before and (b) after annealing at 200°C for 1 h. The

simulation model and the best fit parameters are presented in Figure 4 and Table 2, respectively.

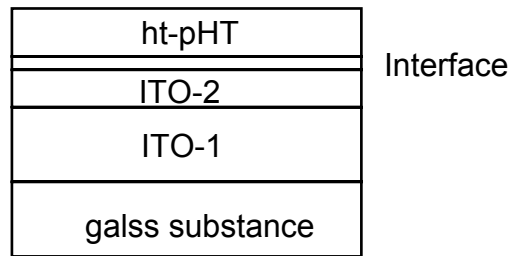


Figure 4. Simulation model for XRR analysis.

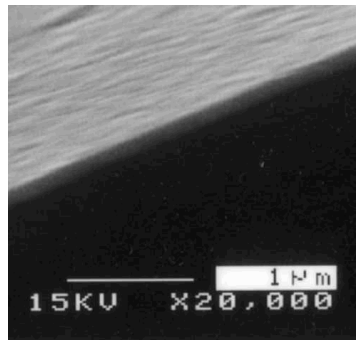


Figure 5. Cross-sectional SEM image of a ht-pHT film on an ITO plate.

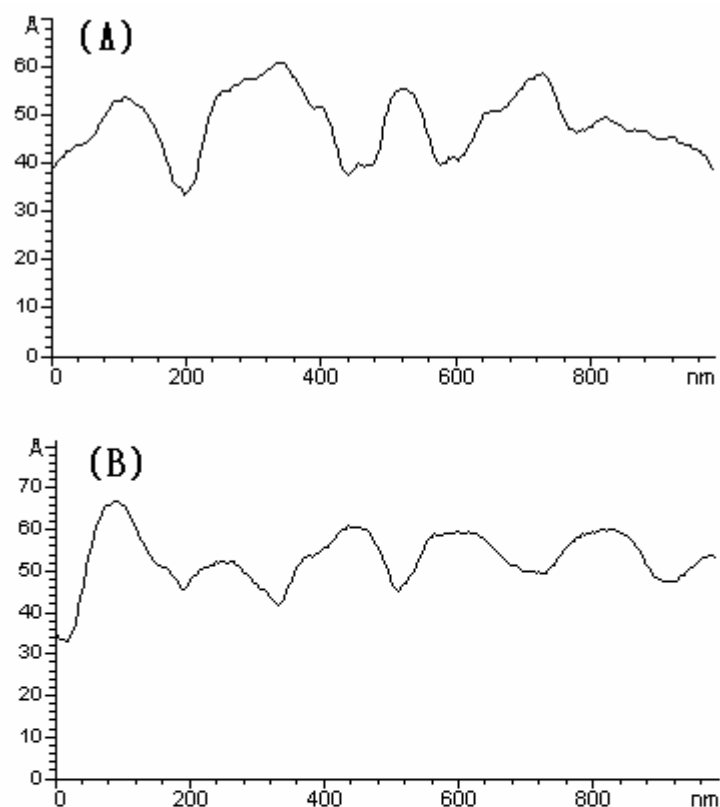


Figure 6. Cross-sectional AFM images of the surface of an ITO plate, (A) before and (B) after annealing at 200°C for 1 h.